50th AIAA Aerospace Sciences Meeting including the New Horizons Forum and Aerospace Exposition
09 - 12 January 2012, Nashville, Tennessee
AIAA 2012-1290

Segmented Ultralight Pre-Aligned Rotor for Extreme-Scale Wind Turbines

Eric Loth[1], Adam Steele[2], Brian Ichter[3]
University of Virginia, Charlottesville, VA 22904

Michael Selig[4]
University of Illinois at Urbana-Champaign, Urbana IL 61801

and Patrick Moriarty[5]
National Renewable Energy Laboratory, Golden, CO

To alleviate the mass-scaling issues associated with conventional upwind rotors of extreme-scale turbines, a downwind rotor concept is proposed which employs fixed blade curvature based on force alignment at rated conditions. For a given peak stress constraint, the reduction in downwind cantilever loads allows reduced shell and spar thickness, and thus a reduced blade mass as compared with a conventional upwind rotor, especially as rotor sizes approach extreme-scales. To quantify this mass reduction, a Finite Element Analysis was conducted for a 10 MW rated rotor based on the NREL offshore 5 MW baseline wind turbine. The results show that this "pre-alignment" yields a net downstream deflection of 32 deg, a downward hub-pitch angle of 6 deg, a 20% increase in blade length (to maintain the same radius as the conventional blade), and a net mass savings of about 50% through decreased shell and spar thicknesses. The pre-alignment may also allow a more straightforward and efficient segmentation of the blade since shear stresses near joints are substantially reduced. Segmenting, in turn, can dramatically reduce costs associated with fabrication, transport and assembly for extreme-scale off-shore systems. The pre-aligned geometric curvature can also help alleviate tower wake effects on the blades since blade tips (where shadow effects can be most problematic) are shifted downstream where the tower wake is weaker. In addition, the portion of the tower that is upstream of the blade tips can be faired with an externally-rotating aerodynamic shroud. Furthermore, the downwind rotor can allow a floating off-shore tri-pod platform to reduce tower weight and yaw-control requirements. A simple economic analysis of the segmented ultralight pre-aligned rotor (SUPAR) concept suggests that the overall system cost savings can be as much as 25%, indicating that more detailed (numerical and experimental) investigations are warranted.

Nomenclature

α	=	angle of attack
B	=	number of rotor blades
β	=	load-path angle
C	=	centrifugal force
D	=	drag force
F_Q	=	torque force
G	=	gravitational force
g	=	gravitational acceleration

[1] Professor, Mechanical and Aerospace Engineering, 122 Engineer's Way., and AIAA Associate Fellow
[2] Research Associate, Mechanical and Aerospace Engineering, 122 Engineer's Way
[3] Undergraduate Researcher, Mechanical and Aerospace Engineering, 122 Engineer's Way
[4] Associate Professor, Aerospace Engineering, 104 S. Wright St., and AIAA Senior Member
[5] Senior Engineer, National Wind Technology Center, and AIAA Associate Fellow

γ = lift over drag ratio
λ = tip speed ratio
L = lift force
m = mass
η = overall mechanical and electrical efficiency of the shaft and generator system
ω = angular velocity
P = power
φ = azimuthal blade angle
R = blade radius
r = radial distance from hub
S = total side force
T = thrust force (downwind aerodynamic force)
τ = torque moment
θ = hub-tilt angle
TSR = tip speed ratio
V = velocity

Subscripts

blade = integrated over blade
cut-in = at cut-in wind speed
cut-out = at cut-out wind speed
down = blade at $\varphi = \pi$ position
o = a reference baseline condition
rated = at rated power conditions
rel = relative to moving blade
rot = rotational
seg = segment of blade (along its length)
up = blade at $\varphi = 0$ position
wind = upstream wind conditions

I. Issues with Extreme-Scale Systems

WIND energy is a growing and critical component of the nation's energy independence path and its drive towards greater environmental stewardship. However, wind energy systems face difficult competition from traditional carbon-based energy sources with respect to cost competitiveness per kW-hr. To counter this problem, many energy systems have increased in size and power in order to achieve utility-scale production and cost efficiencies. As a result, the average wind turbine rated power has increased twenty-fold since 1985 (Fig. 1), with many present large-scale systems averaging 5 MW. Economics of scale and higher winds aloft are driving systems to ever larger sizes. These future "extreme-scale" systems are expected to have power levels of 10-20 MW with rotor diameters on the order of 170-240 m (where the latter is also shown on Fig. 1). As a result, extreme-scale wind turbines would be much larger than any existing airplanes, and furthermore have load distributions that are greater in the outboard section than airplanes. Since torque increases linearly with the turbine power and most of the torque results from the outer blade span, the cantilever loads that must be supported by extreme-scale wind turbines are much larger than those supported by airplanes. For example, a wing of a 747 applies a moment of roughly $3x10^6$ Nt-m on the fuselage at cruise conditions, while a horizontal blade of a 20 MW wind turbine would apply a moment of roughly $3x10^7$ Nt-m on the hub at rated conditions.

These increased cantilever moments make structural design for rotor blades quite difficult. In fact, the scales and loads of an extreme-scale wind turbine are more typical of the largest cable-stayed bridges (Fig. 2). Note that such bridges are designed to use tension cables to avoid the mass and cost inefficiencies of pure cantilever support. This major design shift suggests that conventional rotor design may be problematic and expensive at extreme-scales. In particular, perhaps the two biggest issues associated with cantilever loads for conventional configurations at these scales are the mass of the rotors and fabrication/assembly of an integral (single piece) rotor blade. These two issues are discussed separately in the next two sections.

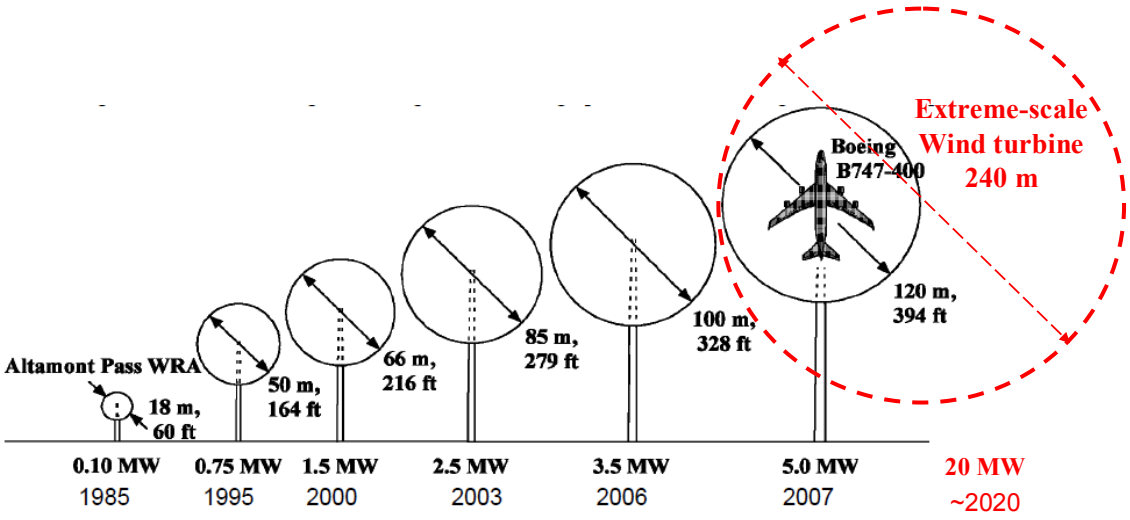

Figure 1. Increase in wind turbine scale and power.[1]

Figure 2. One of the largest cable-stayed bridges located in Charleston, South Carolina[2] *compared with the diameter of a 20 MW wind turbine.*

A. Issues of Rotor Blade Mass at Extreme Scales

One of the most significant challenges associated with extreme-scale systems is blade weight. The rotor blade mass is fundamentally related to the stiffness and structural integrity required to resist the expected peak loads. In resisting these loads, conventional upwind rotors must be structurally designed to limit flexibility so that the blades do not bend downstream and cause a tower strike. Furthermore, the structural design must avoid excessive material stresses and fatigue loading at all expected conditions, as these can result in loss of structural performance or even blade failure. These requirements on rotor stiffness lead to large blade masses and difficult design challenges as noted by Marc Rapin of ONERA: "Wind turbine blades are very rigid. Hence the weight problem in the rush towards giant wind turbines: for 5 MW prototypes, each 61.5-m long blade weighs around 20 tons, which must in turn be supported by a colossal nacelle and tower. So the wind turbine weighs between 400 and 500 tons! That's the limit of what we can manufacture, transport, and predict." [3]

The relationship between blade mass as a function of rotor radius (R) can be estimated theoretically if gravity effects are ignored and the following parameters are held constant: wind speed, tip speed ratio, non-dimensional radial distribution of non-dimensional extracted power, lift and drag coefficients, maximum angle of deflection, material properties and non-dimensional blade structural geometry. In this limit, linearized bending beam theory predicts that the blade mass scales with R^3. However, increased efficiencies with scale, improved structural design over time, as well as use of lighter and stronger materials have resulted in sub-cubic scaling for rotor masses. For example, trends of blade mass for large-scale turbines (defined herein as 1-5 MW) as shown in Fig. 3 indicate an empirical scaling of $R^{2.1}$, while other sources[4] have proposed a scaling of $R^{2.35}$. This scaling is important since the rotor accounts for about 23% of the initial total system cost and many other components of the turbine system increase in scale and cost as the rotor mass increases.[4]

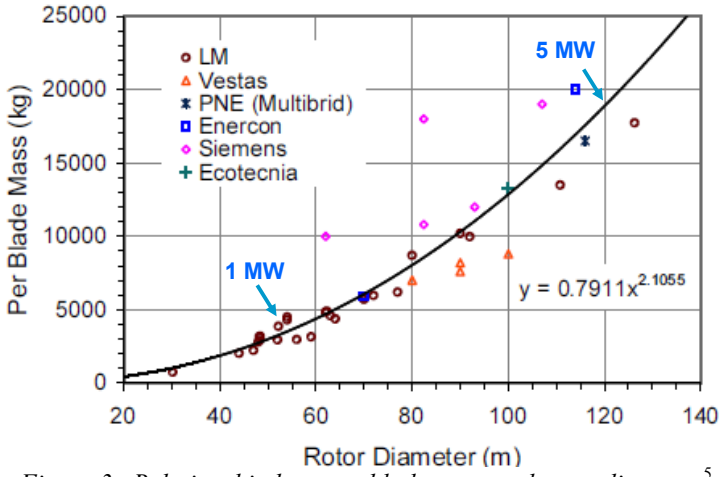

Figure 3. Relationship between blade mass and rotor diameter.[5]

Such empirical scaling estimates indicate that an individual blade for a 20 MW three-bladed system could weigh in excess of 75,000 kg. Furthermore, the importance of gravity loads at extreme-scales may worsen the size dependency on rotor mass beyond that of the scaling associated with the large-scale turbines of Fig. 3. This relationship is due to rated power increasing with swept area (i.e. R^2) whereas blade mass and thus gravity loads increasing at least super-quadratically. As a result, gravity load impact on structural design is relatively small for medium-scale turbines (100 to 1000 kW), moderate for large-scale systems (1-5 MW), and becomes quite substantial for extreme-scale designs. In fact, Hillmer projected that gravity loads become greater than centrifugal and aerodynamic loads once the turbine power exceeds 15 MW ($R > 100$ m).[6] As such, the stresses caused by gravity loads have become a constraining design factor for extreme-scale systems.[1] Thus, concepts to reduce blade mass while maintaining aerodynamic performance, minimizing maintenance, and preventing fatigue is expected to drive future rotor design.

While blade mass reduction can be addressed by using stronger materials, cost constraints generally prevent widespread implementation of this option. For example, carbon fiber material costs can exceed $200/kg while e-glass costs roughly $10/kg. Other options include reducing gust loads through fast-acting control systems (e.g. use of tabs and flaps on the tailing edge of blades), but these may increase fabrication complexity, which again offsets some of the cost savings achieved by a reduction in mass.

As a result, more dramatic design changes have been proposed for future extreme-scale systems. There are several current ventures that seek to upscale traditional horizontal axis designs including the 10 MW Britannia by Clipper Windpower, the Azimit by Gamesa, and the Sea Titan by American Superconductor. The EU-funded UpWind project[7] explored the design limits of up-scaling wind turbines to 20 MW and proposed fore-bending blades with more flexible materials (blades which are pre-bent upstream so that they have more room to deflect downstream at rated conditions) to lower fatigue loads by 10%. An example of this is the LMH64-5 blade, which is an LM Glasfiber Holland B.V. design that is all glass fiber and is pre-bent upstream to avoid tower strikes.[8] The UpWind project also proposed using individual blade control to lower fatigue loads by 20-30% and segmenting the blade in two pieces to allow each to be pitch-controlled separately, which could lower fatigue loads by 15% by allowing faster and more tailored adaption to changes in wind speed and direction.[7]

Other proposed extreme-scale designs are more radical. For example, the Aerogenerator X by Wind Power Limited[9] (Fig. 4a) combines elements of both horizontal and vertical wind turbines and was inspired by sycamore seeds. It employs a V-shaped structure with rotating blades at the end of each arm for off-shore applications. As the wind blows, the blades and arms generate lift to turn the structure at a rate of about 3 revolutions per minute to generate a predicted 10 MW. The Aerogenerator X claims to reduce stress and blade mass by mounting the generator and electronics at the base. However, it may still have the problems of lower efficiency and increased fatigue that have been consistently associated with large-scale vertical axis wind turbines. Another design proposed by NIMROD Energy Ltd is a horizontal axis machine with eight blades[10] as shown in Fig. 4b. The four long and four short blades are supported by a network of external cabling to allow for reduced blade mass by reducing cyclic gravity loads. Power would then be generated non-traditionally via pistons that travel back and forth inside tubes in the blades, compressing air. It is claimed that such a design only becomes feasible at extreme scales 200 meters in diameter and higher where angular rotation is slow enough to allow the pistons to travel the length of the blade.

However, asymmetrically shifting such an extreme amount of weight within the blades may induce complex dynamics and fatigue problems. The blades will also have to be very stiff to allow the piston travel, which may require additional structural mass. Furthermore, most of the cantilever loads are downwind and the proposed external cabling does not support these moments. An even more radical design is proposed by Kite Gen that employs a massive kite-powered carousel[11] (Fig. 4c). At various points around the carousel, high altitude kites are attached and controlled to circle in the air at an altitude of 800 – 1000m. The vertical rotating axis of the structure then activates large-scale alternators that have been geared down to receive the exerted force. At its full capacity the flight of the entire power kites array is guided, so as to turn the carousel at the desired speed to generate power. Thus "blade" mass is significantly reduced since the kites and supporting cables replace the traditional turbine blade, allowing the majority of the high loads to be carried mass efficiently in tension (without a cantilever load). It is claimed that rated power level of 1,000 MW can be reached without significant structural risks with a diameter of approximately 1,600 m. Such a radical design is still in its infancy and several considerable design challenges obviously remain, including issues with kite control and dynamics, carousel structural design and cost, as well as air-space clearance issues for the kites.

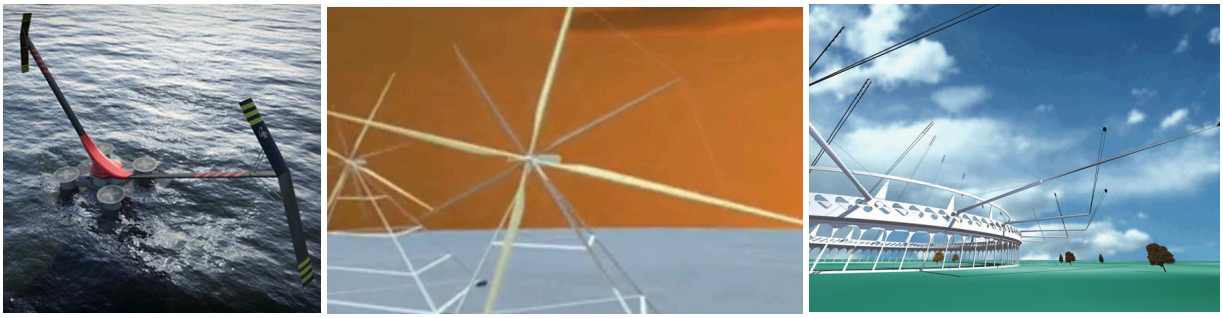

a) b) c)

Figure 4. Conceptual renderings of a) the Aerogenerator X[9] b) NIMROD Energy Ltd's 18 MW design[10], and c) the kite powered carousel by Kite Gen.[11]

While the above concepts, both incremental and radical, hold promise in reducing blade mass to some extent, feasible near-term transformational reduction in blade mass, e.g. 50% or more, may require a new paradigm in rotor design. Adaptable blade geometry may hold the greatest potential toward such an objective. This is not a new concept and in fact has been used on many successful (and unsuccessful) systems. An example of this is the downwind Soft Rotor concept which allowed flexible blades to bend downstream.[12] This downwind system allowed free-yawing to eliminate the need for mechanical yaw control. A two-bladed 15-kW (13 meter diameter) version was field tested where the power and loads were controlled by active stall and coning. Comparison with a similar rigid blade system indicated that rotor loads were reduced by 25-50% during operation as well in a "parked" position in extreme winds. In addition, it was found that aerodynamic efficiency for flexible and coned rotors was approximately equal to that of rigid rotors of the same disk area, i.e. the same radius. While this concept avoided the use of external cables to reduce cantilever loads, the flexible design introduced complexity with respect to blade manufacture and concern with respect to blade cyclic fatigue.

B. Issues with Integral Rotor Blades at Extreme-Scales

Another major problem associated with conventional rotor design at extreme scales is the multitude of issues associated with an integral blade. While an integral design eliminates the mass of joints designed to carry high shear-based cantilever loads, it also introduces other complications for very long blade lengths. In particular, the problems of manufacture, transport and assembly of moderate-scale turbine blades (Fig. 5) will be exacerbated for extreme-scale blades longer than 100 m. The transport and assembly problems will be further compounded for off-shore turbines due to the increased difficulty associated with site accessibility. This is important because off-shore wind energy holds the greatest promise for extreme-scale systems because of the increased and steadier wind speeds available off-shore compared with most on-shore locations. Furthermore, the substantial noise and visual impact of extreme-scale systems will drive their placement away from populated regions. Thus, locations that are "far off-shore" (greater than 10 km) are preferred since noise and visual impact may be negligible to coast-line observers. Far off-shore locations are also less likely to contain aviary flight paths, and thus can ensure very low probabilities of bird strikes, which can reduce the environmental impact of extreme-scale turbines.

Figure 5. Fabrication, transport and assembly of a wind-turbine.[1,13]

Since the future of wind energy penetration for the United States may lie in extreme-scale off-shore turbines, the combination of system size and location will amplify accessibility issues for delivery, construction, and maintenance. Therefore, off-shore extreme-scale systems may require blade segmentation to be cost-effective, and this concept has already been employed for land-based systems. For example, the Enercon 126 (with a rated power of 7 MW with a 126 m rotor diameter) employs segmented blades[14] (Fig. 6) because of the impracticality of transporting complete blades by road. Here, segmentation allows for an erection crew only approximately twice the size needed for a 2 MW turbine[15]. Joining together the segments of each wind turbine blade requires one and a half days per blade. Similarly, a blade insert joint has been designed by Gamesa for a segmented wind turbine blade.[16] This innovation allowed the company to manufacture a 62.5 m wind turbine blade for a 4.5 MW wind turbine with only the logistical constraints of a 2 MW design. Other more radical approaches to blade segmentation exist, such as joining blade segments with truss connections.[17] Unfortunately, segmentation, especially if more than two segments per blade is desired, becomes more complex to design efficiently at extreme-scales in a traditional configuration because of the substantial cantilever loads at the joints. As a result, overall blade mass may increase substantially.

Figure 6. Images of the erection of a 7 MW Enercon 126[14] *showing the segmented blade connection.*[15]

C. Objectives of Present Study

To address the mass and integral-blade design issues associated with conventional rotors at extreme-scales, a rotor is proposed herein which uses a fixed downstream curvature based on force alignment at rated conditions. This "pre-alignment" reduces cantilever loads and thus allows: 1) a substantially reduced mass since stiffness requirements are relaxed, and 2) a more straightforward segmentation since the loads are primarily carried in the tensile mode. A rendering of this segmented ultralight pre-aligned rotor (SUPAR) concept is shown in Fig. 7. The present study of this design is organized as follows: Part II describes the concept of pre-alignment to reduce cantilever loads; Part III provides a computational assessment of the mass savings possible from such alignment;

Part IV discusses the benefits of a segmented rotor blade as well as other system issues including shadow effect; and Part V addresses the potential cost of energy (COE) savings relative to a conventional 10 MW off-shore turbine design.

a)  b) 

Figure 7. Conceptual comparison of: a) a conventional upwind rotor, and b) a downwind aligned rotor (wind direction from left).

II. Pre-Aligned Rotor

A. Pre-Alignment Concept

Similar to the conventional wind turbine design, the oak tree has an integral trunk (that can be approximated as a solid cylindrical beam) that is strong and stiff, though quite heavy. In moderate-speed winds, the oak tree trunk will undergo very little deflection, i.e. it will remain stiff and vertical like the conventional wind turbine configuration (Fig. 7a) that must minimize such deflection to avoid tower strike. This designed stiffness leads to the blade mass scaling problems discussed above. Another issue with a stiff design for trees is that hurricane-level winds can blow and uproot such trees because the aerodynamic forces become too large. This is why oak trees are rare along the shore of coasts which are susceptible to such storms. In contrast, the palm tree's structural system has a segmented trunk that can be approximated as a series of cylindrical shells with a fibrous core. This light-weight shell structure allows high moments of inertia about the trunk axis for a given mass, similar to that used in wind turbine blades with a fiberglass shell and internal foam core. In the face of moderate-speed winds, the flexible living structure of the palm tree can also bend downstream thereby reducing cantilever aerodynamic loads. In extremely high-winds, this flow adaptive characteristic allows the tree to bend all the way to the ground and not be uprooted (Fig. 8).

Figure 8. Palm trees bending due to high-speed winds of a hurricane.[18]

As noted above, the natural aero-elastic design of the palm tree reduces the aerodynamic load with minimal structural mass. This bio-inspiration can be similarly used for the wind turbine to minimize rotor mass by avoiding the conventional stiffness constraint and instead adapting a downwind geometry to align with the load path as shown in Fig. 9. Here it can be seen that the conventional blade loading leads to cantilever forces in the downstream direction. In contrast, the aligned concept employs a geometry that orients the loads along the blade length so that the structural loads primarily act in the tension mode. The resulting load-path angles (β) will vary as a function of radius and azimuthal angle, but these changes are minor. By converting loads to a tensile direction, this concept effectively uses design principles of cabled-stayed bridges (Fig. 2) and the kite rotors (Fig. 4c) to reduce mass by minimizing cantilever-based shear loads. However, the present design is unique in that it avoids direct use of cables to direct loads in the tensile direction, and instead incorporates aeroelastic adaptability bio-inspired by the palm tree. If this alignment is fixed (independent of wind speed) and based on eliminating cantilever loads at the rated condition (where peak loads occur), it is termed herein as a "pre-aligned" rotor. Note that a pre-aligned rotor is easier to design than one that morphs as a function of wind speed.

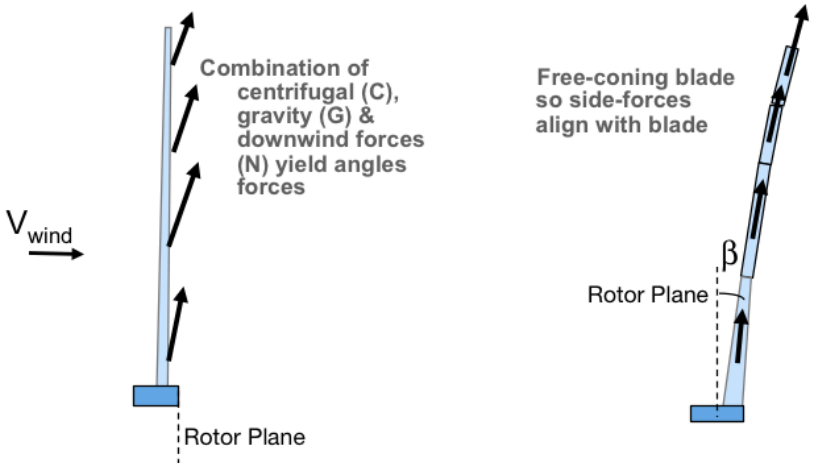

Figure 9. Distribution of forces at rated conditions for a conventional upwind rotor blade and an aligned downwind blade which eliminates downwind cantilever hub moments.

B. Forces and Load Path Angles on a Rotor Blade

To determine the typical angles needed to align a blade with the rated load conditions, one may decompose the forces which act on a turbine blade as shown in Fig. 10. These forces include the gravity force (**G**), the centrifugal force (**C**), the downstream aerodynamic thrust force (**T**), and the in-plane aerodynamic torque-wise force ($\mathbf{F_Q}$). Note that the latter two forces result from the aerodynamic drag force (**D**) and the lift force (**L**).

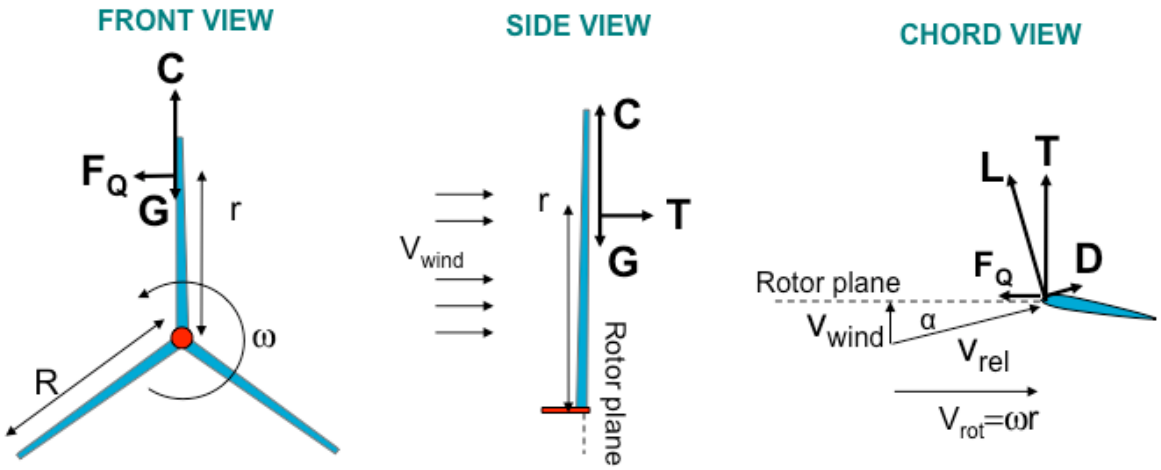

Figure 10. Forces and velocities for a horizontal wind turbine blade.

To compute these forces as a function of the turbine rated power (P_{rated}), one may scale the blade radius (R) and mass (m_{blade}) referenced to a baseline turbine as follows

$$R = R_0 \sqrt{\frac{P_{rated}}{P_{rated,o}}} \tag{1}$$

$$m_{blade} = m_{blade,o} \left(\frac{R}{R_0}\right)^{2.2} \tag{2}$$

The first scaling is the theoretical relation between power and swept area, but the second uses an empirical exponent of 2.2, based on an average of that by Crawford[4] and that of Fingersh[5]. As a baseline system, one may set $P_{rated,o}$ = 5 MW, R_o = 58 m and $m_{blade,o}$ = 18,000 kg based on previous studies.[4,6] The aerodynamic power associated with each blade can then be simply expressed in terms of the number of rotor blades (B) and the overall mechanical and electrical efficiency of the shaft and generator system (η)

$$P_{blade} = \frac{P_{rated}}{\eta\, B} \tag{3}$$

Herein, 3 blades are assumed along with overall efficiency of 90%.

To compute the radial distribution of the blade power and mass, one may discretize the blade into four segments of equal length (ΔR=0.25R) with mean radii for each segment (r_{seg}/R=0.125, 0.3275, 0.625, 0.875). The power production per segment (P_{seg}/P_{blade}) and the blade mass per segment (m_{seg}/m_{blade}) were estimated as shown in Table 1 for four equal segments. These are approximately based on the NREL Unsteady Aerodynamics Experiment (UAE) at the lowest wind speed tested, for which the tip speed ratio was maximized and stall effects were negligible,[19]

Table 1. Blade segment properties

Segment	$\mathbf{r_{seg}/R}$	$\mathbf{P_{seg}/P_{blade}}$	$\mathbf{m_{seg}/m_{blade}}$
1	0.125	5%	46%
2	0.375	20%	26%
3	0.625	35%	16%
4	0.875	40%	12%

The mass distribution allows the gravitational force magnitude to be computed for each segment as

$$G_{seg} = m_{seg} g \tag{4}$$

where **g** is the gravitational acceleration. The centrifugal and torque force magnitudes may also be computed in terms of the rotor angular speed (ω) as

$$C_{seg} = m_{seg}\, \omega^2\, r_{seg} \tag{5}$$

$$F_{Q,seg} = \frac{P_{seg}}{\omega\, r_{seg}} \tag{6}$$

The angular speed can be expressed in terms of the wind speed (V_{wind}) and the turbine power generating conditions (cut-in, rated, and cut-out) and the optimum tip-speed ratio (λ)

$$\omega = 0 \quad \text{for } V_{wind} < V_{cut\text{-}in} \tag{7}$$

$$\omega = \lambda(V_{wind}/R) \quad \text{for } V_{cut-in} < V_{wind} < V_{rated} \tag{8}$$

$$\omega = \lambda(V_{rated}/R) = \text{const.} \quad \text{for } V_{rated} < V_{wind} < V_{cut-out} \tag{9}$$

$$\omega = 0 \quad \text{for } V_{wind} > V_{cut\text{-}out} \tag{10}$$

The tip speed ratio is typically set to a high value to optimize efficiency and estimated herein as λ =7 for off-shore conditions, while the rated wind speed controls the maximum power and is herein set as 14.3 m/s, consistent with a maximum tip speed of 100 m/s. The cut-in and cut-out speeds are based on operational efficiency and safety and are herein estimated as 4 m/s and 28.6 m/s.

To compute the aerodynamic downwind force, one may compute the relative segment velocity (V_{rel}) and its approximate angle of attack (α) relative to the rotor plane (Fig. 10) as

$$V_{rel}^2 = V_{wind}^2 + \left(\omega\, r_{seg}\right)^2 \tag{11}$$

$$\alpha \sim \sin^{-1}\left(\frac{V_{wind}}{V_{rel}}\right) \tag{12}$$

Applying small angle approximations, the downwind normal thrust force can then be computed in terms of the lift-to-drag ratio (γ=L/D) as

$$T_{seg} \sim F_{Q,seg}\left(\frac{\cos\alpha+\gamma\sin\alpha}{\sin\alpha-\gamma\cos\alpha}\right) \tag{13}$$

To optimize performance, the lift to drag ratio is typically maximized and is estimated herein as 20 (though this value is not critical to the results presented below). To find the net forces for a blade, the four segments are simply summed, e.g. $G = \Sigma G_{seg}$.

The net forces based on the above analysis are shown in Fig. 11 as a function of wind speed. It can be seen that the torque-force is the smallest of all the forces (even though this is the only one that produces power). The peak loads can be seen to occur at the rated wind speed where the normal force is highest. Thus, the rated conditions experience the highest steady-state blade stresses.

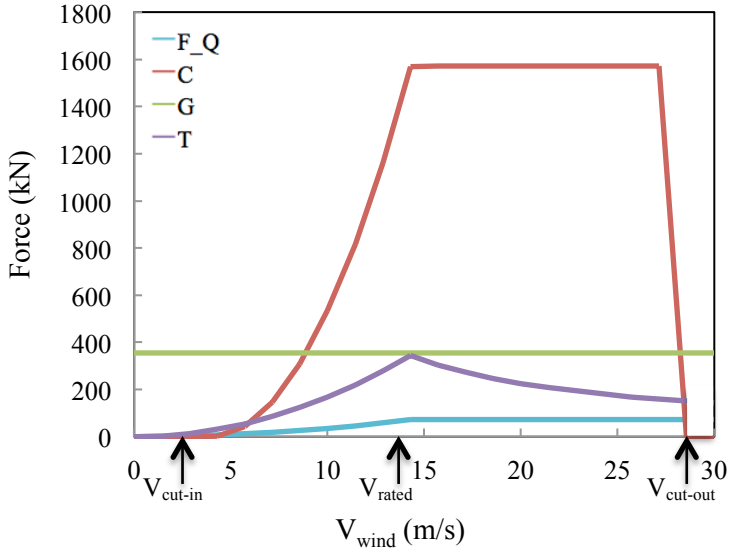

Figure 11. Total forces on a rotor blade pointed upward (φ=0) as a function of wind speed for a 10 MW rated turbine with a conventional upwind vertical rotor.

One may estimate the net load-path angle (β) in terms of these net forces and the azimuthal blade angle (φ, defined as 0 for a blade that is pointed vertically upwards and π for a blade that is downwards) as:

$$\beta = \tan^{-1}\left(\frac{T}{C-G\cos\varphi}\right) \tag{14}$$

This load-path angle is shown in Fig. 12 for the blade pointed upwards (β_{up}, where φ = 0) and downwards (β_{down}, where φ = π) as a function of turbine rated power. For moderate-size turbines (less than 1 MW), the load-path angle at rated conditions is small (typically less than 5 deg.) so that some of this can be accommodated by aeroelastic deflection for an upwind conventional rotor. This indicates that aligned blades do not benefit small systems. However, for large- and extreme-scale turbines the load-path angles can be large, e.g. more than 20 degrees for a 20 MW system. This trend of increasing β with increasing P is a result of size-scaling for a constant tip-speed ($\omega \sim R^{-1}$) such that $C \sim R^{1.2}$ (Eqs. 2 and 5), $T \sim R^{2}$ (Eqs. 1, 6 and 13), while $G \sim R^{2.2}$ (Eqs. 2 and 4).

Since cantilever loads are more significant at extreme-scales, alignment allows a larger reduction in the moments experienced by the blade. (per Fig. 9). Furthermore, aligning the blade geometry at these large angles downstream necessitates a downwind rotor. *Thus, scaling will drive extreme-scale systems to downwind aligned rotors.* One may also note that there is a significant difference in the upwards and downwards load-path angles in Fig. 12, which is due to the increased importance of gravity loads at extreme-scales. Additional differences in these load path angles can occur if there is a vertical wind-shear across the rotor causing higher wind speeds at higher altitudes. To avoid cyclic appearance of cantilever loads while maintaining a fixed rotor geometry with respect to the hub, the hub axis can be tilted relative to the horizon as a function of wind speed by θ as shown in Fig. 13. If a two-bladed design is used, this tilting can instead be achieved by teetering the rotor. For two- or three-bladed

designs, individual pitch control and/or trailing edge surfaces (flaps or tabs) may accommodate tilt-pitch coupling as well as rapid changes in wind angle or speed caused by gusts. It should be noted that rotor speeds above rated conditions will result in only a small reduction in the load path angles, such that pre-alignment at rated conditions will be nearly ideal. For rotor speeds below rated conditions, the load path angles will generally not be aligned with those at rated conditions, but at these lower speeds the loads on the blades are substantially reduced (Fig. 11) so that the adaption is not needed to avoid peak stresses on the blades.

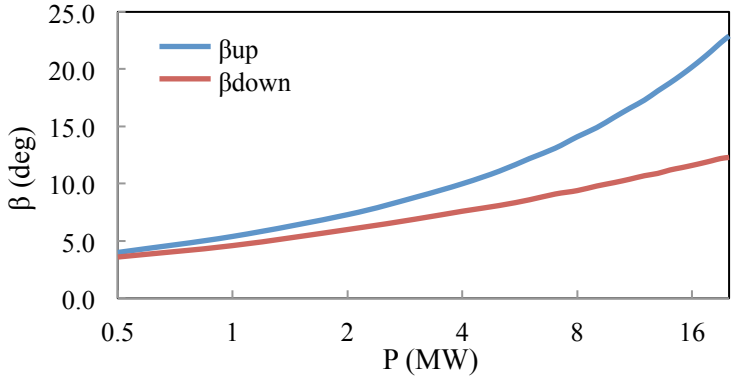

Figure 12. Average load-path angles (β) at rated conditions as a function of rated turbine power (P_{rated}).

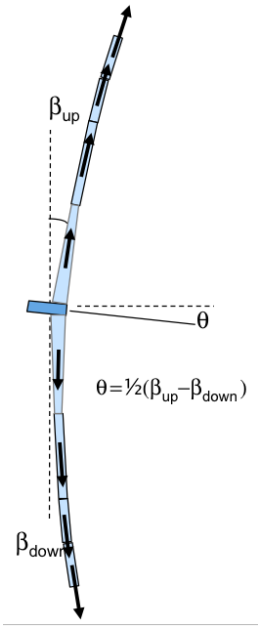

Figure 13. Load path and hub angles for a two-bladed, three-segment downwind force-aligned rotor .

III. Ultralight Rotor Finite Element Analysis

A. Conventional (Baseline) Blade Mass and Design for a 10 MW Rotor

To provide a comparison to the ultralight concept (to be presented in section D) for an extreme-scale system, a conventional 10 MW turbine design was first created. The blade structural design is based on the National Renewable Energy Laboratory (NREL) offshore 5 MW baseline wind turbine.[20] This data was then scaled to a 10 MW design with a radius of 82 m.[6] The scaled data used for the model is summarized in Table 2.

The NREL 5 MW turbine specifies the airfoils at specific nodes along the blade, as are shown in the right column of Table 2. The hub of the blade is modeled as a cylinder, which at 15% of the blade radius transitions into a 40%-thick, Delft University DU40 airfoil. The 40% thickness airfoil then transitions to a thinner airfoil and at three-quarters of the blade radius becomes a NACA 64, 18%-thick, airfoil. The blade remains a NACA 64 airfoil until the tip. The chord distribution was obtained by using the same non-dimensional chord distribution as that of the NREL 5

MW that has a maximum chord length at approximately 25% of the blade radius.[20] The airfoil distribution, airfoil thickness, and blade twist are shown in Fig. 14.

Table 2. Blade geometry for a scaled 10 MW off-shore wind turbine

Node	Radius [m]	Chord Length [m]	Blade Twist [deg]	Angle of Attack at Rated Conditions [deg]	Airfoil
1	3.81	4.61	13.31	58.60	Cylinder
2	7.45	5.02	13.31	44.13	Cylinder
3	11.09	5.42	13.31	33.14	Cylinder
4	15.63	5.93	13.31	23.43	DU40
5	21.09	6.05	11.48	17.47	DU35
6	26.54	5.80	10.16	13.57	DU35
7	32.00	5.53	9.01	11.02	DU30
8	37.45	5.22	7.80	9.50	DU25
9	42.91	4.88	6.54	8.67	DU25
10	48.36	4.56	5.36	8.20	DU21
11	53.82	4.24	4.19	8.04	DU21
12	59.27	3.92	3.13	8.01	NACA64
13	64.73	3.60	2.32	7.90	NACA64
14	70.18	3.28	1.53	7.91	NACA64
15	74.73	3.01	0.86	8.01	NACA64
16	78.36	2.72	0.37	8.10	NACA64
17	82.00	1.85	0.11	7.99	NACA64

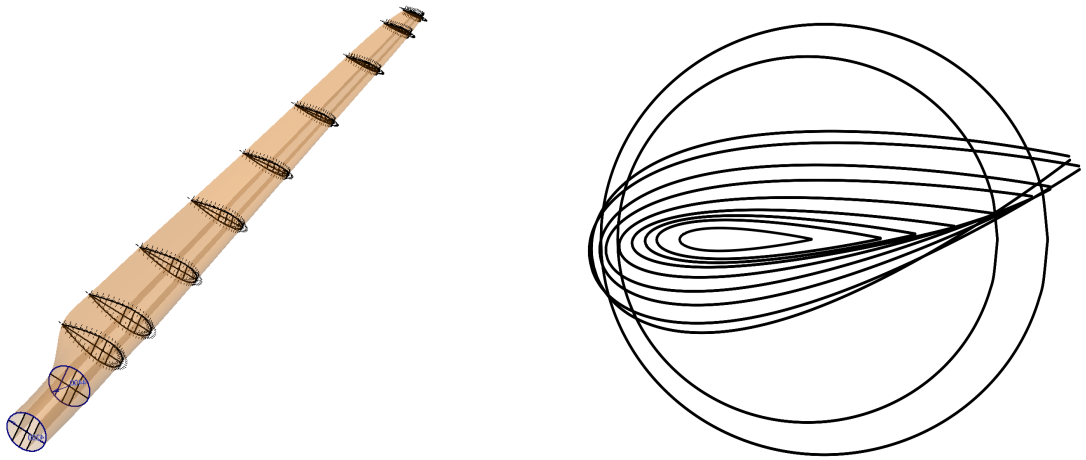

a) b)

Figure 14. a) Airfoil distribution along the blade length showing 11 discrete radial stations, and b) airfoil geometry and blade twist at these same stations.

Data for the shell thickness and material properties were not included in the NREL 5 MW turbine report, so they were determined using known industry practices and scaling approximations. The blade mass was estimated as 35,800 kg, assuming a scaling of $R^{2.2}$ and a baseline blade mass of 18,000 kg at 60 m radius. For the design, the entire blade (outer shell, spar caps, and shear webs) was modeled as a uniform material based on E-LT-5500 fiberglass. The modulus of elasticity was specified as 41.8 GPa, the Poisson's ratio as 0.28, and the density as 1920 kg/m^3.[21] Knowing the material density, the blade mass, and non-dimensional blade mass distribution (based on the NREL 5 MW turbine), the thickness of the shell could be calculated. Since this analysis resulted in a nearly linear

decrease in thickness as a function of radial position, the design was simplified to be linear as shown in Fig. 15 and as consistent with other designs.[20]

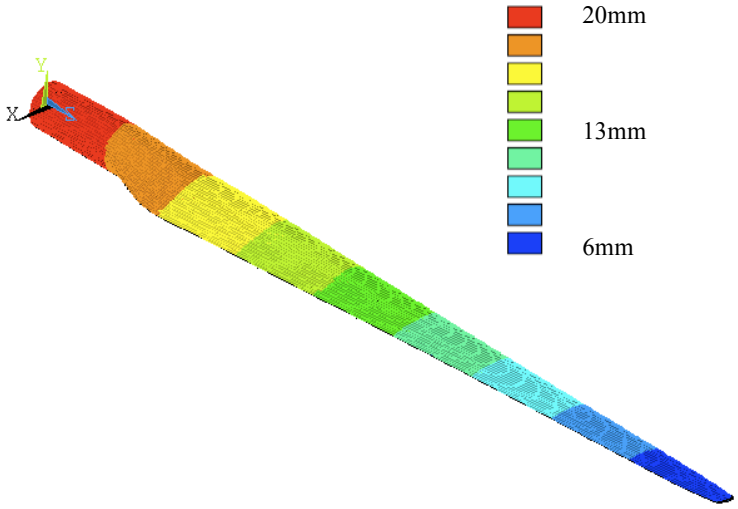

Figure 15. Blade thickness contours along the blade.

The internal geometry was based on a simplified version of conventional wind turbine blade designs as shown in Fig. 16. The shear webs refer to the spars running down the length of the blade, while the spar caps refers to the section between the two shear webs. The shear webs were placed a constant distance apart, resulting in a constant width spar cap.[21] The shear webs were located 0.5 m forward and 1 m aft of the airfoil location of maximum thickness. The thickness of the shear webs was prescribed as a constant 7 mm, based on the constant thickness of the Sandia 100 m all-glass baseline wind turbine blade shear webs.[21] The thickness of the spar cap was prescribed as a constant 15 mm. This value also helped avoid stress hot spots throughout the blade when loaded at rated conditions.

a)

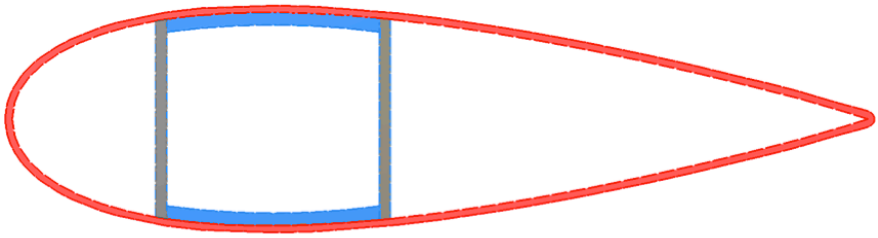

b)

Figure 16. a) The spar cap (blue) width along the length of the blade, and b) an airfoil cross section with two shear webs and spar caps (blue).

B. Finite Element Analysis for Conventional Blade

To determine the stresses expected on a conventional 10 MW extreme-scale turbine blade, Finite Element Analysis (FEA) was used through ANSYS at rated conditions. The non-dimensional power distribution as a function of radius was estimated based on previous computational and experimental data[19,22] as shown in Fig. 17. This distribution was then scaled to match the necessary torque for a power output of 10 MW. Using the same rotor and tip speeds described in Part IIB, the downstream forces were calculated from the torque force (F_Q) and the angle of attack.. The centrifugal and gravitational forces were applied using ANSYS's built-in inertial loading functionality.

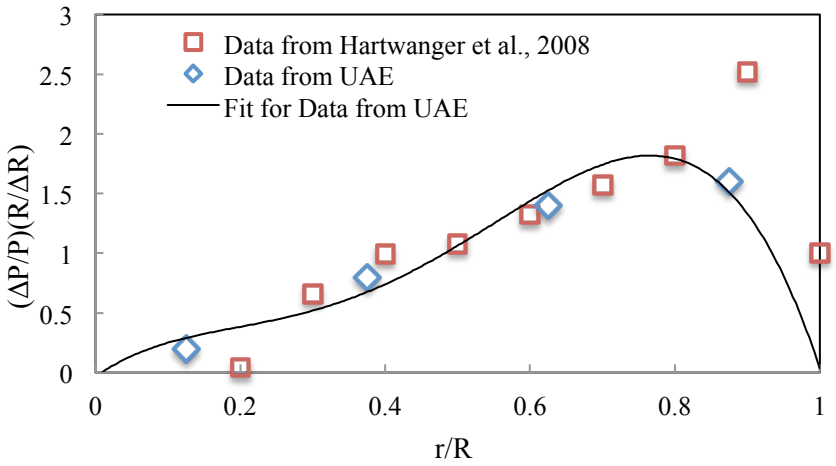

Figure 17. Radial power distrubtion from computational analysis[22] and the UAE experiment at maximum λ.[19]

To perform the FEA, a mesh was created with ANSYS. The model was meshed using shell elements (SHELL181) because of the extremely small thickness compared with the overall blade size (Fig. 18). The maximum element size was set to 0.5 m within ANSYS, which resulted in a mesh of 12,713 elements. In order to apply the aerodynamic forces to the mesh, the force distributions were applied with the force functions found above via surface elements (SURF154) overlayed on each mesh element. The aerodynamic surface elements have zero thickness and are non-structural, thus they do not effect the inertial loadings or the stress results.

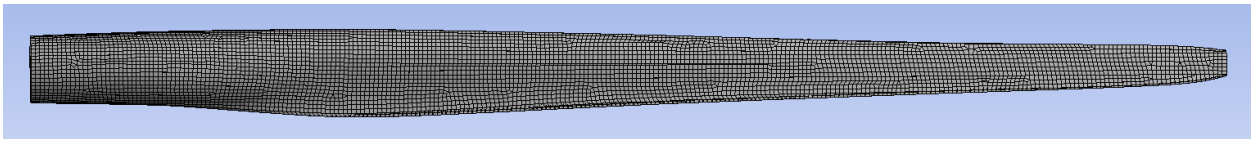

Figure 18. Surface finite element mesh for conventional blade.

The FEA Von Mises stresses for the 10 MW conventional blade at rated conditions are shown in Fig. 19. The stresses were calculated for the blade in the upright (φ=0) position in which gravity acts in the opposite direction to the centrifugal force, in the sideways (φ=π/2) position in which gravity acts in the torque-wise direction, and in the downward (φ=π) position in which the gravitational force acts in the same direction as the centrifugal force. It was found that the maximum Von Mises stress was 112 MPa and occurred at the sideways position. The peak Von Mises stress was 108 MPa for the up position and 109 MPa for the down position. However, the average Von Mises stress found for all three positions was about 60-65 MPa. The maximum variation in stress between the three positions was only 4%. This finding shows that while cyclic moments arise due to gravity loads, these represent small portions of the total stress at rated conditions since aerodynamic and centrifugal forces dominate.

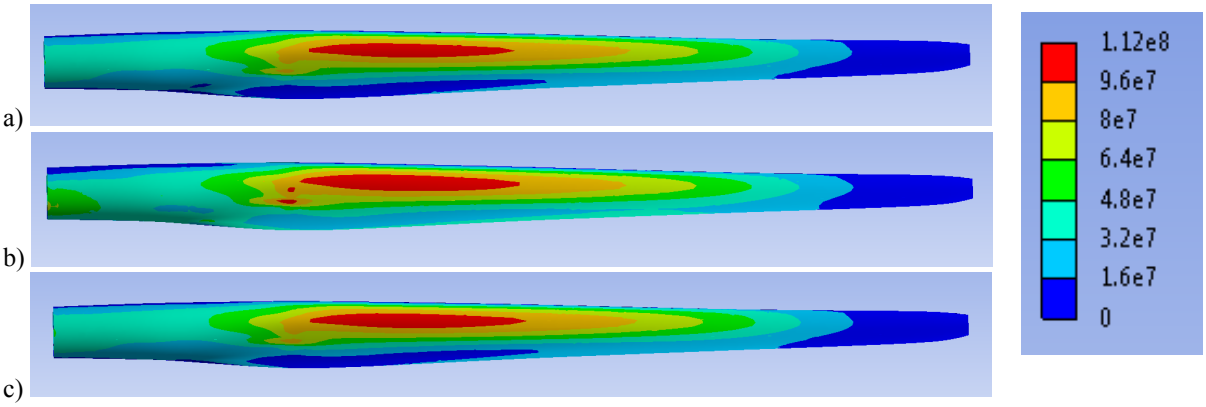

Figure 19. Von Mises stresses in MPa for the conventional blade at rated condition when instantaneously located in the following positions: a) φ=0, b) φ=π/2, and c) φ=π.

C. Finite Element Analysis for Fixed-Mass Aligned Blade

To determine the stresses expected on a fixed-mass aligned downstream blade, a 10 MW aligned blade was created. The mass, thickness, and geometry were held constant and the same aerodynamic forces were applied as used for the conventional 10 MW blade. The only difference was that the aligned blade included downstream curvature. In order to determine the alignment angles, the blade was segmented into four sections. For each segment, the total aerodynamic, centrifugal, and gravitational forces were calculated and assumed to act at the center of each section. Using the force values, the angle at each joint was set so that the net downstream moment at the node points was zero, as shown in Fig. 20a. Once the necessary angles for each of the four joints were found, the geometry was created to match each joint angle. The resulting shape and computational mesh are shown in Fig. 20b, where it can be seen that the blade geometry can be approximately represented as downwind coned. The detailed deflection angle is shown in Fig. 21, where a range from 16-19 deg over the blade radius can be observed.

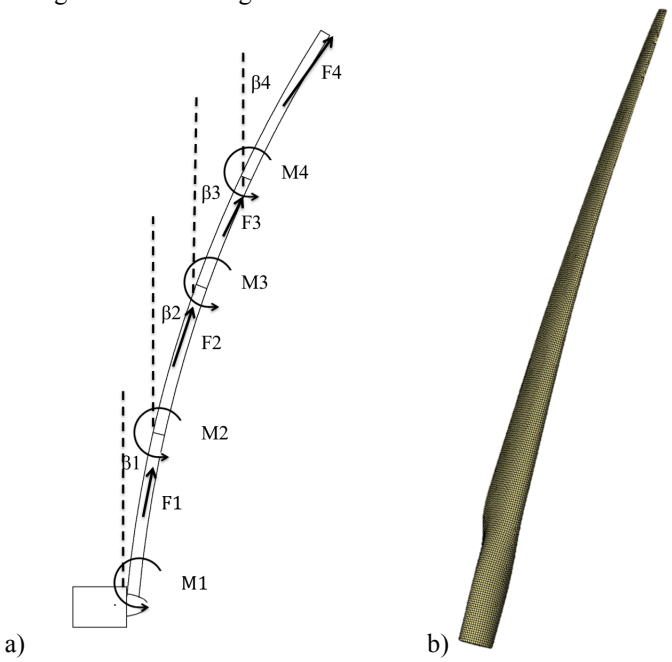

Figure 20. a) Method to ensure zero moment nodes, and b) resulting downstream blade curvature.

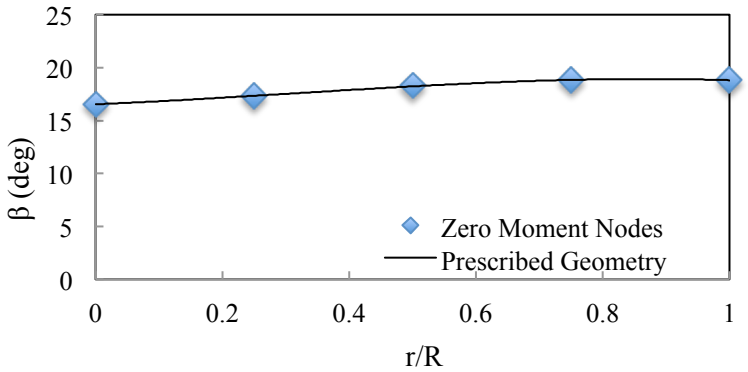

Figure 21. Deflection angle at each node and the resulting fit vs. the radial position for fixed-mass and fixed-length.

FEA was then used in order to determine the stresses in the aligned blade. A mesh of 14,997 shell elements was created in ANSYS again with a maximum element size of 0.5 m (Fig. 20b). Applying the aerodynamic, centrifugal, and gravitational forces using the same method as for the conventional blade, the Von Mises stresses shown in Fig. 22 were calculated. The peak Von Mises stress found was 19 MPa (an 82% stress reduction compared with conventional) and the average stress was 9 MPa (a 85% stress reduction compared with conventional). This demonstrates the substantial benefit of alignment in reducing stresses, and thus stiffness requirements on the blade. It should be noted that the swept area has been reduced by 9% for this case since blade length was kept fixed.

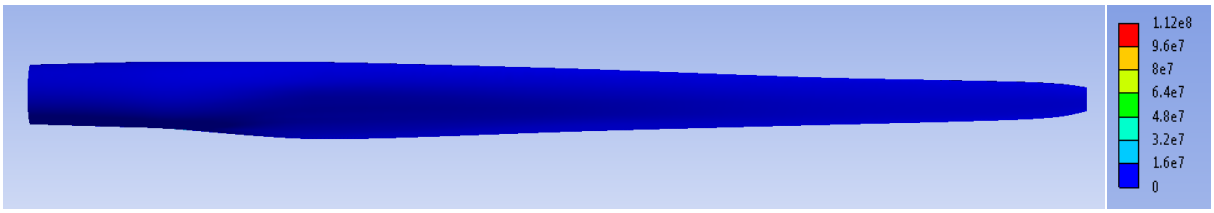

Figure 22. Von Mises stresses in MPa for fixed-mass blade aligned at rated conditions for φ=0.

D. Finite Element Analysis and Design for Ultralight Aligned Blade

To determine the mass savings expected on an aligned downstream blade with the same swept area and thus rated power of a conventional blade, the shell was reduced to a constant 6 mm for the entire blade length (Fig. 23a). In order to save mass, the spar cap thickness was reduced to a constant 8 mm, as its primary function is to increase stiffness, a constraint that can be relaxed with this downwind design.[21] The thickness of the shear webs was reduced to a constant 4 mm of uniaxial material. However, because the torque force remained constant with this thickness decrease, it was necessary to add a trailing edge reinforcement to improve torque-wise stiffness.[21] The trailing edge reinforcement had a constant thickness of 16 mm and was located along the entire blade's trailing edge with a width of 5% of the chord length. In order to avoid a resultant decrease in effective radius, the blade length was increased by 20% so the total swept areas and rated power was equal to the conventional blade. These changes resulted in an overall mass reduction, compared with the conventional blade, of 54%. The alignment of the blade was then recalculated for the new centrifugal and gravitational forces as shown in Fig. 23b. Analyzing this reduced mass blade at rated conditions, it was found that with the blade in the upwards position (φ = 0) the maximum Von Mises stress was 67 MPa and the average Von Mises stress was 26 MPa (Fig. 23c). With the blade in the sideways position (φ = π/2) the maximum Von Mises stress was 121 MPa (located on the inner surface of the blade) and the average Von Mises stress was 52 MPa (Fig. 23d). It is important to note that when the blade is in the sideways position (φ = π/2) the gravitational and torque forces add to each other, creating the highest torque-wise cantilever loads and thus the highest experienced stress. Some additional adjustment may be needed to bring the peak stresses downward and to account for gust loads, but these results generally indicate that mass reductions on the order of 50% are possible.

a)

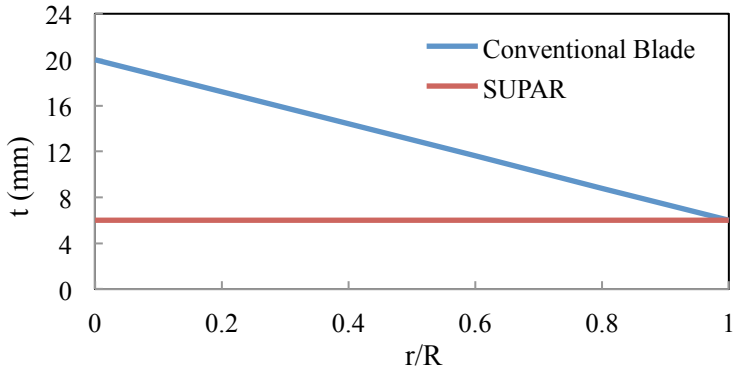

b)

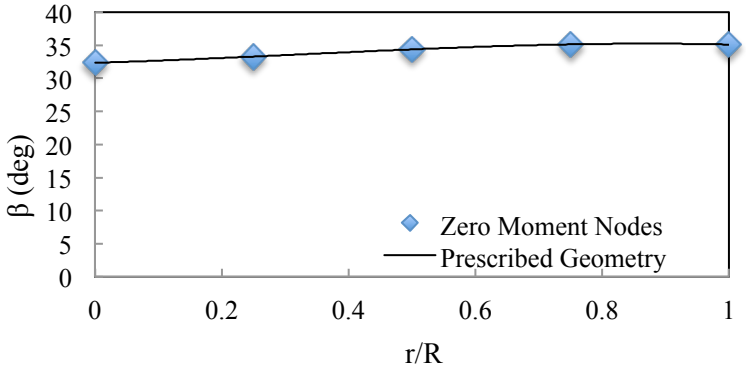

c)

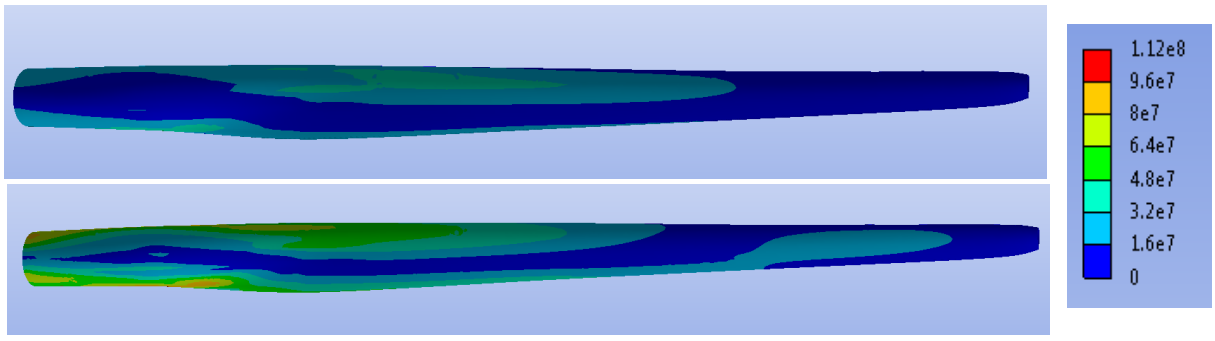

d)

Figure 23. a) Conventional and ultralight blade thickness as a function of radial position, b) alignment angles vs. radial position, c) Von Mises stresses in MPa for a reduced mass aligned blade with conventional blade radius at φ=0, and d) at φ= π/2.

The results of the three test cases are shown in Table 3. Compared to the conventional vertical blade, the "Fixed-Mass Pre-Aligned" blade has much lower stress levels but the combination of fixed length and downstream curvature reduced the blade radius (and the commensurate reduction in swept area would then reduce its rated power). However, the "Ultralight Pre-Aligned" blade uses a lower shell thickness allowing it to have mass reductions on the order of 50% while maintaining a radius and stress levels consistent with a conventional blade. This indicates that the large rotor blade mass reductions are possible while still maintaining the conventional swept area and avoiding any increase in maximum structural stresses. Note that rotor pre-alignment indicates a fixed geometry for all wind speeds (it does not morph) so that cantilever loads are only completely eliminated at rated conditions. However, at speeds other than rated conditions, the downwind loads are reduced (Fig. 11).

Table 3. Stress analysis results for 10 MW blades at rated conditions

Blade Configuration	Peak Von Mises Stresses [MPa]	Average Von Mises Stresses [MPa]	Mass [Mg]	Radius [m]
Conventional	112	62	35.6	82.0
Fixed-Mass Pre-Aligned	19	9	35.9	78.1
Ultralight Pre-Aligned	121	50	16.5	82.0

IV. Segmentation and Shadow Effects

As mentioned in Part II, the present concept takes inspiration from the engineering design of a cable-stayed bridge (Fig. 2) and the bio-design of palm tree (Fig. 8) in order to align aerodynamic, gravity, and centrifugal forces in the tensile direction. The downstream curvature ensures that moments are eliminated along the entire length of the blade at the highest load conditions, so downstream cantilever loads are minimized. The focus of loads in the tensile direction allows segmentation design to be simplified because high shear loading does not need to be communicated across the segments. For example, cables are easily joined because they are simply in tension, where aircraft wing joints require more complicated and heavier joint designs. This blade segmentation aspect can be especially transformative with respect to manufacturing, transporting, and repairing such systems as described in Part IIB. This modularity, coupled with the reduced overall system weight can breakdown barriers inherent to increasing the scale of current turbine designs, as will be described in terms of a cost model in Part V.

However, one common concern about using a downwind rotor is the wake effects of the tower on the blade. These can be problematic as they induce unsteadiness in blade loading that can lead to blade fatigue. However, they can be mitigated in two ways with the SUPAR concept. Firstly, the tower can be aerodynamically faired as shown in Fig. 24. This can have a substantial impact since the drag (and wake of an airfoil) can be many times less than that of a cylinder.

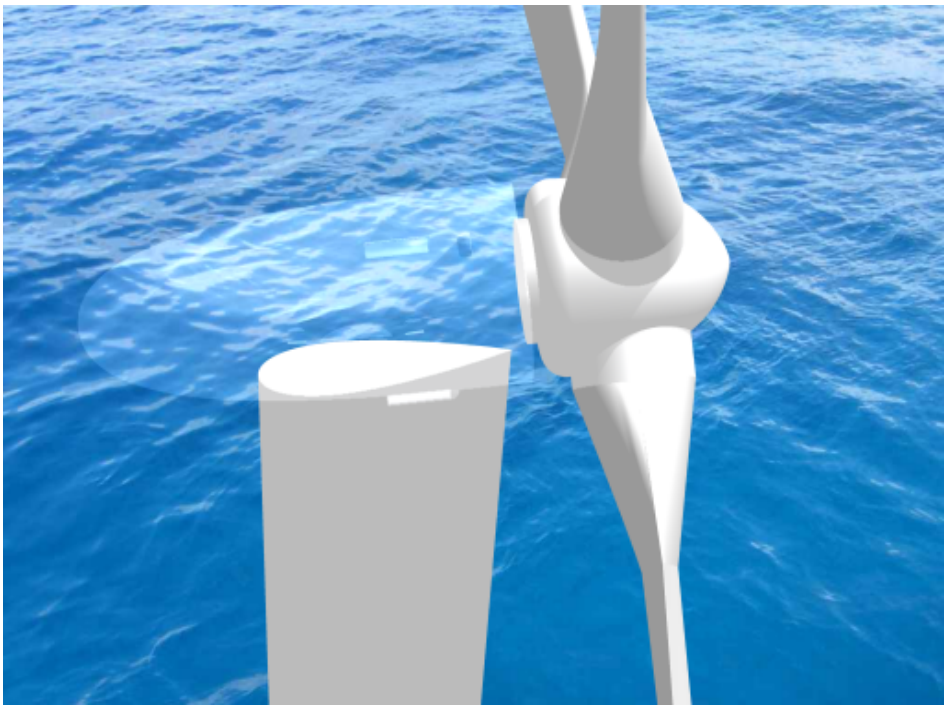

Figure 24. Aerodynamic shroud around the tower for reduced tower wake effects on the blades.

The shroud can be set to externally rotate around a fixed cylindrical structure. The shroud rotation can be passive by allowing aerodynamic forces to align in the proper downstream direction. Since the wake effects are strongest near the outer portion of the blade (where most of the torque and downwind loading occurs), the aerodynamic shrouding may only be required for the section of the tower that are just upstream of the outer blade passage. Furthermore, the geometric downwind curvature also helps alleviate the tower shadow wake effects since the blade tips (where the effect can be most problematic) are shifted far downstream of the tower from pre-alignment. Active yaw control requirements may also be significantly reduced as a result of this downwind design.[12] For very deep waters (>60 m), a downwind rotor could also allow for a floating tripod system as shown in Fig. 25. The upstream floating pod could be cabled below to the sea floor so the thrust force aligns the turbine to the wind (self-yawing). Such a tripod platform (vs. a single column tower) may also help reduce wake effects since the increased stiffness associated with a broader platform allows smaller elements. This could also reduce tower mass since columnar designs at large scales can become costly and large (Fig. 6).

In addition, a morphing concept could be used where the blade alignment need not be fixed for rated conditions and instead the blades would be allowed to have semi-free flapping but with the curvature associated with rated alignment. For speeds significantly below rated conditions, the blades could be fixed on the vertical plane in order to maximize the swept area allowed with the longer length blades. As the wind speed approaches rated conditions, the blades could be gradually released in semi-alignment to reduce stresses. For rated speeds and above, the blades could be fully-aligned, though a dashpot-damper system may be needed to avoid problematic dynamics. Finally, at speeds significantly above cut-out conditions, the stopped blades could be closed-up towards the horizontal to allow a stow configuration for hurricane level winds.

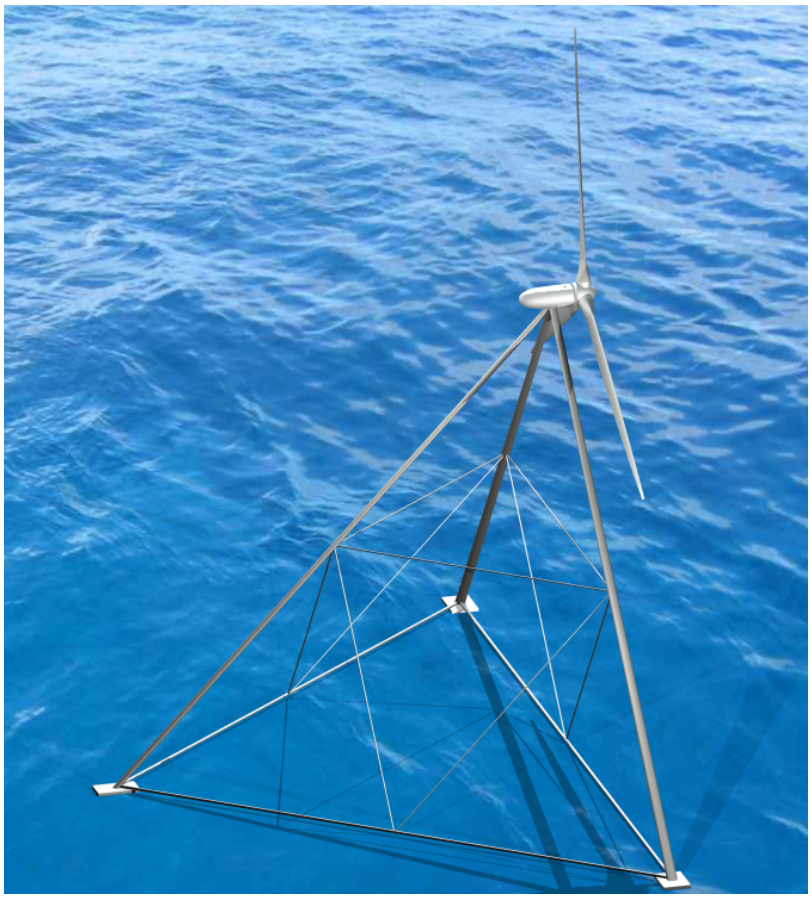

Figure 25. Tripod floating concept (pre-alignment aspects not shown).

V. Impact of SUPAR Concept on Cost of Energy

To illustrate the potential COE reductions possible with a next-generation offshore wind turbine, the SUPAR configuration has been compared with a baseline turbine design using the NREL Wind Turbine Design Cost and Scaling Model.[23] The NREL model defines a permanent magnet direct-drive (PMDD) 10 MW offshore turbine reference configuration, which was selected as the baseline for this cost analysis. For offshore applications, the model assumes an annual average wind resource of 9.16 m/s at 50 m above water level. Tables 4 and 5 show the input values chosen in the cost model where dark gray cells indicate parameters that changed as a result of SUPAR. It was also assumed that a 54% reduction in blade mass allows for a 30% reduction in hub mass and tower mass (due to reduced inertial dynamics). An increase in nacelle mass to incorporate an aerodynamic shroud may be balanced by the decrease in yaw drive requirements. As a first order approximation, it was assumed that a percentage reduction in mass led to the same percentage reduction in cost, e.g. a 54% reduction in blade mass led to a 54% reduction in blade cost. Finally with respect to station costs, it was assumed that blade segmentation combined with such mass reduction led to a 40% reduction in costs related to turbine transportation, port and staging equipment, monopile foundation, and turbine installation. Such cost modifications are first-order approximations and accurate cost estimate changes would require detailed design analysis. In particular, changes due to shadow effects (which could require some increased structural mass) are not included but neither are potential changes in the tower from a column to a tripod system of Fig. 25 (which may lead to even more dramatic reductions in tower mass and assembly cost).

Table 4. Operating parameter inputs for NREL Wind Turbine Design Cost and Scaling Model

	Offshore 10 MW Turbine
Turbine	Idealized Turbine power
Land Based or Offshore Selection	2
Machine Rating (kW)	10000
Rotor Diameter (m)	175
Hub Height (m)	120
Wind Speed Class (50 m)	9.16
Altitude Above Mean Sea Level (m)	0
Max Rotor Cp	0.482
Max Tip Speed m/s	80
Max Tip Speed Ratio	8
Wind Farm Size in MWs	250
Total Non-Drivetrain Losses	10%
Availability	95%

Table 5. Initial capital costs for NREL Wind Turbine Design Cost and Scaling Model

	Baseline Component Mass (kg/kW)	**SUPAR Component Mass (kg/kW)**	**Baseline Component Costs $/kW**	**SUPAR Component Costs $/kW**
Rotor	**62**	**39**	**428**	**255**
Blades	31	14	289	133
Hub	20	14	55	38
Pitch mechanism & bearings	7	7	82	82
Spinner, Nose Cone	4	4	2	2
Drive train, nacelle	**153**	**153**	**922**	645
Low speed shaft, bearings, & gearbox	87	87	121	121
Generator, elec. connections, yaw drive	37	36	700	680
Main frame & hydraulic cooling system	28	28	90	90
Nacelle cover, breaks & HS coupling	1	2	20	40
Control, Safety System, and Monitoring	**0**	**0**	**10**	**10**
Tower	**115**	**80**	**373**	**261**
Marinization	**0**	**0**	**173**	**173**
NET MASS / TURBINE CAPITAL COST	**328**	**272**	**1,905**	**1,364**
Monopile Foundation/Support Structure			604	362
Turbine Transportation and Installation			2,215	1,329
Port and Staging Equipment			40	24
Electrical Interface/Connect			606	606
Permits, Engineering, Site Assessment			55	55
Scour Protection & Access Equipment			120	120
Surety Bond			166	166
BALANCE OF STATION COST			**3,806**	**2,663**

Table 6 summarizes the result of this analysis showing a 30% reduction in turbine capital cost and a 30% reduction in balance of system cost, while operations and maintenance cost as well as levelized replacement cost were assumed to remain constant. These improvements resulted in a total system cost reduction of 25%, directly resulting from a 54% reduction in blade mass from force-aligned segmented blades. These cost savings are realized because pre-alignment reduces rotor mass while segmentation and modularity simplifies fabrication, transportation,

and assembly. Such significant cost savings may break down many of the remaining barriers inherent to extreme-scale off-shore wind turbines.

Table 6. Wind energy systems Cost of Energy Summary for Off-Shore Turbines

Representative Categories	10 MW Baseline	SUPAR	Improvement
Turbine Capital Cost ($/kWh)	$0.037	$0.027	28%
Balance of System Cost ($/kWh)	$0.075	$0.052	30%
Operations & Maintenance Cost ($/kWh)	$0.018	$0.018	0%
Levelized Replacement Cost ($/kWh)	$0.004	$0.004	0%
Total System ($/kWh)	**$0.135**	**$0.102**	**25%**

VI. Conclusions

There are many challenges posed by extreme-scale systems that will need to be addressed through technological innovation and demonstration in the next 10-20 years. For such systems, the SUPAR concept may alleviate the mass-scaling problems and fabrication complexity associated with conventional upwind rotor design. The ultralight aspect is achieved by a downwind fixed blade curvature based on force alignment at rated conditions. This curvature ensures that downstream moments (caused by aerodynamic, gravity and centrifugal forces) are eliminated all along the blade path at the highest load conditions. Forces are thus primarily carried through tension, thereby eliminating any rated cantilever loads, except for those in the torque-wise, power-generating direction. By eliminating the cantilever loads at rated conditions, the stiffness requirements are substantially relaxed. As the rotor size increases, this translates into greater percentage reduction of blade mass relative to a conventional upwind rotor of the same swept radius and same structural stresses. *Such mass savings are a result of the size-scaling which drives extreme-scale systems to larger load-path angles and thus more towards downwind aligned rotors.*

To quantify this mass reduction, a Finite Element Analysis was conducted for a 10 MW rated rotor based on the NREL offshore 5 MW baseline wind turbine. The results showed that an ultralight pre-alignment design yields a net downstream deflection of 32 deg, a 20% increase in blade length (to maintain the same effective radius as the conventional blade), and a net mass savings of about 50% through decreased shell and spar thicknesses. Another key benefit of the force alignment is that it allows a more straightforward and efficient segmentation of the blade since shear stresses at joints are greatly reduced. Finally, a cost of energy analysis of this concept was performed using the NREL Wind Turbine Design Cost and Scaling Model for off-shore applications. The results indicate that the reduced rotor mass and potential savings with transportation and installation may yield a 25% cost reduction as compared to a conventional upwind rotor for the same rated power level. A summary of the chief potential benefits of the SUPAR concept is listed in Table 7. However, the quantitative improvements are only approximate (especially with respect to COE changes). Therefore, further detailed experimental and numerical investigations are required to provide improved accuracy for determining whether this concept is as viable and efficient as suggested by the initial estimates of this study. In particular, effects of blade segmentation, gust loading, pitch control, energy capture, and shadow effects should be considered. In addition, a morphing concept could be used to allow: 1) increased swept area and power at speeds below rated conditions, 2) better alignment at speeds above rated conditions, and 3) stow capability for hurricane level winds.

Table 7. Performance comparison of conventional rotor and SUPAR

	Conventional Rotor	SUPAR
Swept Radius	82 m	82 m
Rated Power	10 MW	10 MW
Rotor Mass	36.5 Mg	16.5 Mg
Cost	$0.135	$0.102
Yaw Control	Active	Reduced
Shadow Effects	None	Mitigated

VI. References

[1]Ashwill, T.D. "Materials and Innovations for Large Blade Structures: Research Opportunities in Wind Energy Technology," *AIAA/ASME/ASCE/AHS, ASC Structures, Structural Dynamics, and Materials Conference*, AIAA Paper 2009-2407, 2009.

[2]Bbatsell, "Arthur Ravenel, Jr. Bridge" [online] 2007, en.wikipedia.org/wiki/Arthur_Ravenel_Jr._Bridge [retrieved June 2011].

[3]Marc Rapin of ONERA, 2009, http://www.onera.fr/zoominthelab/38-wind-turbines-computers-in-the-fields.php [retrieved June 2011]

[4]Fingersh, L.J., Hand, M., and Laxson, A., *Wind Turbine Design Cost and Scaling Model*, Golden, CO: NREL Technical Publishing, NREL/TR-500-40566, 2006.

[5]Crawford, C., "The Path from Functional to Detailed Design of a Coning Rotor Wind Turbine Concept", *CDEN/C2E2 Conference*, Winnipeg, Manitoba, July 22–24, 2007

[6]Hillmer, B, T. Borstelmann, A.P. Schaffarczyk and L. Dannenberg, *Aerodynamic and Structural Design of MultiMW Wind Turbines beyond 5 MW*, Journal of Physics, Conf. Series, 75, 012002, 2007.

[7]Fichaux, N., Beurskens, J., Jensen, P. H., Wilkes, J., Frandsen, S., Sørensen, J. D., Eecen, P., Malamatenios, C., Gomez, J. A., Hemmelmann J., van Kuik, G., Bulder, B., Rasmussen, F., Janssen, B., Fischer, T., Bossanyi, E., Courtney, M., Giebhardt, J., Barthelmie, R., and Holmstrøm, O., "Design limits and solutions for very large scale wind turbines", *EWEA 2011*, Brussels, Belgium, March 2011.

[8]Kooijman, H. J. T., Lindenburg, C., Winkelaar, D., and van der Hooft, E. L., "Aero-elastic modelling of the DOWEC 6 MW pre-design in PHATAS," DOWEC-F1W2-HJK-01-046/9, 2003.

[9]Wind Power Limited, "Wind Power's 10MW Aerogenerator X aims to provide 1GW of power by 2020," [online], 2011, http://www.windpower.ltd.uk [retrieved 20 December 2011].

[10]NIMROD Energy Ltd., "UK Startup Targets Reducing Wind Energy Costs by Four Times and Wind Energy Storage by Five Times," *Next Big Future* [online], 2010, http://nextbigfuture.com/2010/03/uk-startup-targets-reducing-wind-energy.html [retrieved 20 December 2011].

[11]Kite Gen, "Kite Gen Carousel," [online], 2011, http://www.kitegen.com/en/ [retrieved 20 December 2011].

[12]Rasmussen, F., Petersen, J.T., Volund, P., Leconte, P., Szechenyi, E., and Westergaard, C. "Soft Rotor Design for Flexible Turbines", Riso National Laboratory, Roskilde, Denmark, Contract JOU3-CT95-0062.

[13] Coker, C. "Wind Turbine Blade" [online] www.flickr.com/photos/caveman_92223/3348491430/ [retrieved June 2011].

[14]Enercon and Terex-Cranes, "Crane power enables wind power in large turbine assembly," *EU Infrastructure* [online], 2009, http://www.euinfrastructure.com/article/Crane-power-enables-wind-power-in-large-turbine-assembly/ [retrieved 20 December 2011].

[15]Thomas, J., "New Record: World's Largest Wind Turbine (7+ Megawatts)," *Metaefficient* [online], 2008, http://www.metaefficient.com/news/new-record-worlds-largest-wind-turbine-7-megawatts.html [retrieved 20 December 2011].

[16] Arocena de la Rua, I., Pascual, E., and Collado, S. US Patent Application for "Blade insert." Application Number 12/492,163, filed 26 June, 2009.

[17]Arendt, C., Baker, P., and Myles, L. International Patent Application for "Segmented wind turbine blades with truss connection regions, and associated systems and methods", Application Number PCT/US2011/037815, filed 24 May 2011.

[18] NOAA, "Pam Tree Bending" [online], www.photolib.noaa.gov/ [retrieved June 2011].

[19]Simms, D., Schreck, S., Hand, M and Fingersh, L.J. "NREL Unsteady Aerodynamics Experiment in the NASA-Ames Wind Tunnel: A comparison of Predictions to Measurements" NREL/TP-500-29494, June 2001.

[20]Jonkman, J., Butterfield, S., Musial, W., and Scott, G., *Definition of a 5-MW Reference Wind Turbine for Offshore System Development*, Golden, CO: NREL Technical Publishing, NREL/TR-500-38060, February 2009.

[21]Griffith, T. and Ashwill, T., *The Sandia 100-meter All-glass Baseline Wind Turbine Blade: SNL100-00*, Albuquerque, NM: Sandia National Laboratories, SAND2011-3779, 2011.

[22]Hartwanger, D., and Horvat, A., "3D Modeling of a Wind Turbine Using CFD", *NAFEMS Conference*, United Kingdom, 2008.

[23]Fingersh, L.J., Hand, M and A. Laxson "Wind Turbine Design Cost and Scaling Model" NREL/TP-500-40566, December 2006.